

Simplified Method for Evaluating the Flight Stability of Liquid-Filled Projectiles

Daniel J. Weber*

U.S. Army Edgewood Research, Development, and Engineering Center,
Aberdeen Proving Ground, Maryland 21010

This paper describes a modification to the tricyclic theory to include the effect of a liquid payload on the motion and stability of the projectile. The influence on the projectile's motion by the liquid payload is similar to the Magnus effect. A computer program has been developed that determines the complex projectile motion using either theoretical estimates of liquid-fill characteristics or experimental results obtained from a test fixture for nonrigid payloads. Preliminary stability assessments for liquid-filled projectiles can be made rapidly and provide a means of determining the relative importance between the aerodynamic and liquid-fill characteristics on the projectile's flight stability. Flight stability predictions show good agreement with flight tests of liquid-filled, 155-mm projectiles.

Nomenclature

C_{m_q}	= dynamic stability derivative coefficient
C_{m_α}	= static stability derivative coefficient
C_{m_δ}	= aerodynamic trim derivative coefficient
$C_{NRP_{\theta p}}$	= nonrigid payload side moment coefficient
$C_{n_{\beta p}}$	= Magnus moment derivative coefficient
d	= reference diameter, m
I	= transverse moment of inertia, kg-m ²
I_x	= axial moment of inertia, kg-m ²
$K_{1,2,3}$	= length of nutation, precession, and aerodynamic trim arms, deg
M_{LRM}	= liquid-induced roll moment, N-m
M_{LSM}	= liquid-induced side moment, N-m
M_{LSM_θ}	= liquid induced side moment due to θ , N-m/rad
$M_{LSM_{\theta p}}$	= liquid induced side moment due to θ and p , N-m-s/rad ²
$M_{p\beta}$	= Magnus moment due to β , N-m-s/rad ²
M_q	= pitch moment due to q , N-m-s/rad
M_α	= pitch moment due to α , N-m/rad
$M_{\dot{\alpha}}$	= pitch moment due to $\dot{\alpha}$, N-m-s/rad
M_δ	= pitch moment due to δ , N-m/rad
$m_{1,2}$	= complex roots to differential equation
$N_{1,2,3}$	= constants in linearized aeroballistic equation
p	= spin rate, rad/s
q	= pitch rate, rad/s
q'	= dynamic pressure, $\frac{1}{2} \rho V^2$, N/m ²
S	= reference area, m ²
s_g	= gyroscopic stability factor
t	= time, s
V	= velocity, m/s
α	= angle of attack, deg
α_0	= initial angle of attack, deg
$\dot{\alpha}_0$	= initial time rate of change of α , deg/s
β	= angle of sideslip, deg
β_0	= initial angle of sideslip, deg
$\dot{\beta}_0$	= initial time rate of change of β , deg/s
Δt	= tricyclic theory time step, s
δ	= control deflection angle, deg
ϵ	= complex angle of attack, $\beta + i\alpha$, deg
θ	= test fixture nutation angle, analogous to ϵ , deg

$\lambda_{1,2}$	= nutation and precession damping exponent (real part of m)
ν	= kinematic viscosity, cSt
ρ	= atmospheric density, kg/m ³
σ_N	= total angle of attack in sun-fixed axes (yawsonde data), deg
τ	= defined by Eq. (7)
ϕ	= roll rate measured in sun-fixed axes (yawsonde data), rev/s
$\omega_{1,2}$	= nutation and precession frequency (imaginary part of m), rad/s

Introduction

THE tricyclic theory provides a relatively complete solution to the linearized aeroballistic equations that describe the free-flight motion of a rolling vehicle. Until now, the tricyclic theory only considered the influence of the projectile's physical properties (diameter and moment of inertia) and aerodynamic characteristics (static and dynamic stability derivatives, Magnus, and aerodynamic asymmetries) in determining the flight motion.¹ Flight dynamicists using this theory can parametrically analyze the flight characteristics of a projectile to determine which factors have the greatest influence on its stability. The influence of the payload on the projectile's flight motion is not considered. This assumption is correct for solid payloads but not for liquid payloads. It has been shown experimentally, theoretically, and through firing tests that liquid payloads (i.e., liquid fills) can cause flight instabilities.² Currently there are several analytical and computational methods available to determine the effects of a liquid payload on the flight stability of a projectile.³⁻⁵ The drawbacks to these methods are that they are complicated to use, they require large computers and a substantial amount of computer time, and the results are sometimes difficult to interpret. By including the liquid payload effects in the tricyclic theory, many of these drawbacks are eliminated. The tricyclic theory is easy to use, employs conventional aeroballistic and aerodynamic definitions and nomenclature, can run on many different types of computers, and executes quickly, and the results are displayed in a graphical format for easy interpretation.

It should be noted that the modified tricyclic theory will simulate the flight motion of a projectile with a wide range of liquid payload viscosities as well as projectiles with free-moving mechanical payloads. The only requirement is the ability to determine the payload-induced side moment. For liquid payloads, the resulting side moments have been determined from theories, laboratory experiments, and flight tests for payload viscosities ranging from 1 cSt (water) to infinite (solids). In this study, the payload viscosity range was limited from 1000 to approximately 200,000 cSt because of the readily available flight test results.

Presented as Paper 92-0650 at the AIAA 30th Aerospace Sciences Meeting, Reno, NV, Jan. 6–9, 1992; received March 21, 1992; revision received Dec. 10, 1992; accepted for publication Jan. 26, 1993. This paper is declared a work of the U.S. Government and is not subject to copyright protection in the United States.

*Aerospace Engineer, Aerodynamic Technology Team. Member AIAA.

Conventional Tricyclic Theory

The conventional tricyclic theory employs an aeroballistic axes system and solves the aeroballistic equations of projectile motion by simplifying them to a single linear differential equation. By solving this differential equation, the angular motion of a projectile can be determined for a given set of flight conditions. The linearizing assumptions on which this theory is based are small angles, constant aerodynamic coefficients, nonthrusting vehicle, rotation and mass symmetry (no dynamic imbalance), and a rigid body. Applying these assumptions to the aeroballistic equations of motion yields the following linear second-order differential equation:

$$\ddot{\epsilon} + N_1 \dot{\epsilon} + N_2 \epsilon = N_3 e^{ip\tau} \quad (1)$$

where $\epsilon = i\alpha + \beta$ is the complex total angle of attack, and N_1 , N_2 , and N_3 are constants defined as

$$N_1 = \left(-ip \frac{I_x}{I} - \frac{M_q + M_{\dot{\alpha}}}{I} \right) \quad (2)$$

$$N_2 = \left(-ip \frac{M_{p\beta}}{I} - \frac{M_{\alpha}}{I} \right) \quad (3)$$

$$N_3 = i \left(\frac{M_{\delta}}{I} \right) \quad (4)$$

Solving Eq. (1) yields

$$\epsilon = K_1 e^{m_1 \tau} + K_2 e^{m_2 \tau} + K_3 e^{ip\tau} \quad (5)$$

where K_1 , K_2 , and K_3 are the nutation, precession, and trim arms, respectively; K_1 and K_2 are constants determined from the initial boundary conditions, and K_3 is found from the aerodynamic trim moment. The mass properties and aerodynamic characteristics of the projectile are used to determine the frequencies and damping ratios for both the precession and nutation arms. The frequencies $\omega_{1,2}$ and the damping ratios $\lambda_{1,2}$ are determined from the following expression:

$$m_{1,2} = \lambda_{1,2} + i\omega_{1,2} = \left[\left(\frac{M_q + M_{\dot{\alpha}}}{2I} \right) (1 \pm \tau) \pm M_{p\beta} \frac{\tau}{I_x} \right] + i \left[\frac{pI_x}{2I} \left(1 \pm \frac{1}{\tau} \right) \right] \quad (6)$$

where the subscripts 1 and 2 denote the nutation and precession motion, respectively. The variable τ is defined by

$$\tau = \frac{(pI_x/2I)}{[(pI_x/2I)^2 - (M_{\alpha}/I)]^{1/2}} = \frac{1}{[1 - (1/s_g)]^{1/2}} \quad (7)$$

and s_g is the gyroscopic stability factor that for a spin-stabilized projectile must be greater than 1 for stability. The variable s_g is expressed as

$$s_g = \frac{(pI_x/2I)^2}{(M_{\alpha}/I)} \quad (8)$$

At this point, the rigid-body (i.e., no liquid payload) assumption still holds. The next step is to relax the rigid-body assumption and include the effects on the projectile's angular motion due to a liquid payload.

Modified Tricyclic Theory to Include Liquid-Fill Effects

To incorporate the liquid-fill effects into the tricyclic theory, the liquid payload moment must be included in the mathematical expressions of the theory. It has been shown through the derivations of the moment equations^{3,6,7} that the liquid-induced side moment always acts about an axis that is located in the total-angle-

of-attack plane (i.e., coning angle) and perpendicular to the spin axis. This moment tends to yaw the projectile out of the total-angle-of-attack plane and has exactly the same moment orientation as the Magnus moment. Also, like the Magnus moment, the liquid side moment is a function of both spin and total angle of attack (i.e., coning angle). The intent is not to redevelop these equations but instead to use the similarity between the Magnus and liquid-fill terms in the tricyclic theory for liquid-filled projectiles. That is, both moments are functions of the projectile's spin rate and total angle of attack and affect the equations of motion in a similar manner. The liquid payload moment is also a function of the projectile's nutation rate. In the tricyclic theory, both the spin and nutation rates are constant throughout the entire simulation. To include the liquid-fill effects, the Magnus moment term in Eq. (6) for nutation only, m_1 , is modified by adding the liquid side moment; m_2 as described by Eq. (6) is unchanged. Thus, m_1 from Eq. (6) becomes

$$m_1 = \left[\dots + (M_{p\beta} + M_{LSM_{\theta p}}) \frac{\tau}{I_x} \right] + i \dots \quad (9)$$

It is important to emphasize that $M_{LSM_{\theta p}}$ is only applied to the damping of the nutational motion of the projectile. There are a couple reasons for defining Eq. (9) in this manner. First, $M_{LSM_{\theta p}}$ is a function of rotational frequency, and generally for a spin-stabilized projectile the nutation frequency is an order of magnitude greater than the precession frequency. Thus, different values of $M_{LSM_{\theta p}}$ would have to be applied for the nutation and precession frequencies, respectively. Since the value of $M_{LSM_{\theta p}}$ for precession is much smaller than that for nutation, the contribution of $M_{LSM_{\theta p}}$ for precession is ignored. Also, a spin-stabilized projectile is stable in the precessional mode; thus the small contribution of $M_{LSM_{\theta p}}$ to precession will only increase its damping, making the projectile slightly more stable in precession.

The other reason for defining Eq. (9) in the form shown deals with the assumption that $M_{LSM_{\theta p}}$ only affects the dynamic stability. This assumption is valid for projectiles that have a small length-to-diameter ratio, i.e., artillery shells. For projectiles with a large length-to-diameter ratio, i.e., missiles, the liquid payload can affect the static stability $C_{m_{\alpha}}$ of the projectile and, thus, the nutation and precession frequencies. In the present study only projectiles with small length-to-diameter ratios were considered.

Induced Liquid Side Moment Coefficient

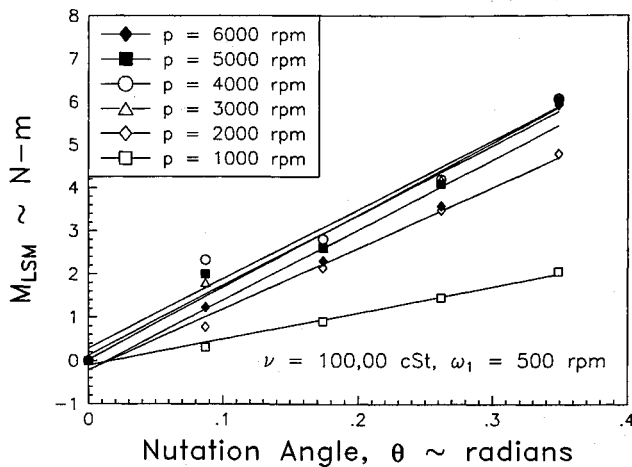
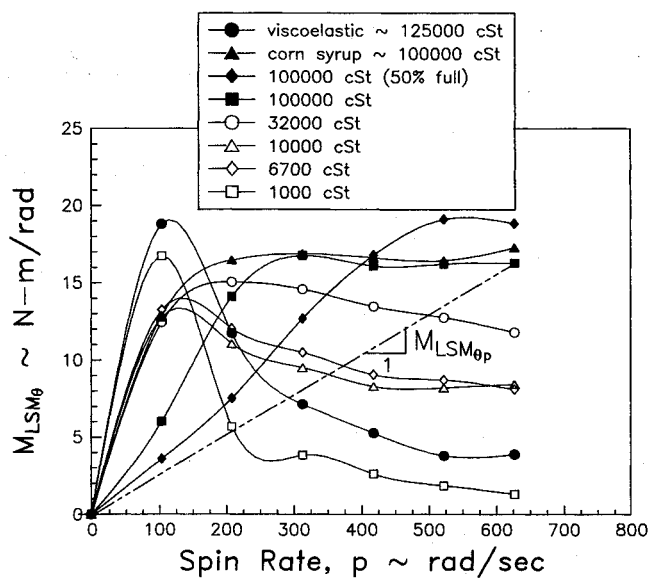
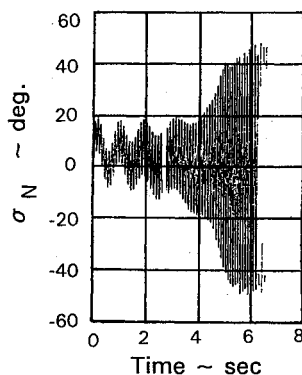
All aerodynamic terms used in the theory are entered as coefficient derivatives, and the liquid side moment must also be converted to a similar coefficient. The liquid side moments required to determine the coefficients can be either estimated by computer programs or measured directly using a laboratory test fixture for nonrigid payloads. The latter method was used for this paper. The laboratory test fixture for nonrigid payloads simulates the spin and nutational motion of a full-scale 155-mm projectile payload canister. For a given liquid payload viscosity, test fixture results are available for nutation rates of 200–500 rpm in 100-rpm increments, nutation angles of 5–20 deg in 5-deg increments, and spin rates of 1000–8000 rpm in 1000-rpm increments that encompass a nominal range of flight projectile conditions.⁸

The test fixture measures the liquid roll moment acting on the payload canister. The liquid side moment is related to the liquid roll moment by the following relationship:⁷

$$M_{LSM} = -\frac{M_{LRM}}{\tan \theta} \quad (10)$$

Thus, the test fixture liquid roll or despin moments were converted to liquid side moments for this analysis using Eq. (10).

By using the assumption that the liquid payload only influences an artillery projectile's damping and not its angular frequency, the conventional tricyclic theory (i.e., solid body or $M_{LSM_{\theta p}} = 0$) can be used to determine the nutation rate. For this study, a 155-mm projectile at transonic flight conditions was used in the tricyclic theory to determine the nutation frequency, $\omega_1 = 500$ rpm. There are two reasons for using a 155-mm projectile and the transonic flight con-

Fig. 1 M_{LSM} vs θ for constant spin rates.Fig. 2 M_{LSM} vs p for various fluid viscosities.Fig. 3 σ_N vs time for round E1-9394.

ditions. First, there are available flight test results for this configuration. Second, a transonic flight provides the least amount of aerodynamic stability to a projectile, and thus large angles of attack that increase the liquid-fill effect can be experienced. Knowing the nutation rate of the projectile, the liquid-induced side moments that relate to this motion are then selected. Figure 1 shows a typical plot of M_{LSM} vs nutation angle θ , which was obtained from the test fixture for various constant spin rates p , a silicone fluid of $\nu = 100,000$ cSt, and an $\omega_1 = 500$ rpm. The resulting curves of M_{LSM} vs θ for constant spin rates are fitted to straight lines with slopes being

denoted $M_{LSM\theta}$. Figure 2 shows $M_{LSM\theta}$ vs p for a range of different fluid viscosities.

To be consistent with the definition of the Magnus coefficient, the derivative $M_{LSM\theta p}$ must be determined from Fig. 2. A problem occurs at this point in the determination of $M_{LSM\theta p}$ because for a given fluid the derivative is not constant with spin rate. This problem is avoided because of a basic assumption of the tricyclic theory that the spin rate is constant. To obtain the correct liquid-fill moment for a given set of flight conditions, $M_{LSM\theta p}$ is assumed to be the slope of the straight line through the origin and the intersection of the $M_{LSM\theta}$ vs p curve at the desired projectile spin rate. As an example, the slope of the dash line in Fig. 2, for fluid of 100,000 cSt and a spin rate of 628 rad/s (6000 rpm), represents the value of $M_{LSM\theta p}$ for this fluid and spin rate. This approach is reasonable due to the constant spin rate assumption and because M_{LSM} is a linear function of θ . What is important is that $M_{LSM\theta}$ corresponds to the correct spin rate of the particular flight condition being simulated. With $M_{LSM\theta p}$ evaluated, the final form of the liquid side moment term was determined by the following equation that is analogous to the Magnus coefficient:

$$C_{NRP\theta p} = \frac{2V M_{LSM\theta p}}{q'Sd^2} \quad (11)$$

For each of the fluids shown in Fig. 2, values of $C_{NRP\theta p}$ were determined and are listed in Table 1.

Comparison of Tricyclic Theory to Flight Test Results

As a demonstration of the modified tricyclic theory's ability to predict the stability of a projectile, a comparison will be made with the results of flight tests of liquid-filled, 155-mm projectiles. The tabulated test results are provided in Table 2⁹ and Table 3.¹⁰

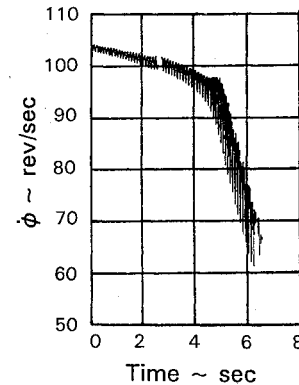
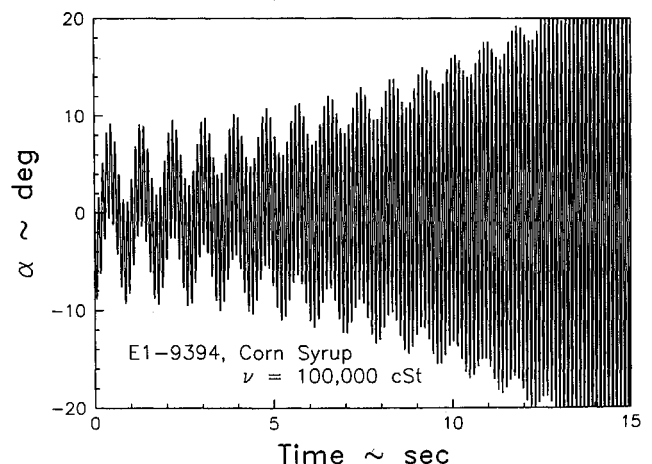
Fig. 4 ϕ vs time for round E1-9394.Fig. 5 Tricyclic flight simulation for round E1-9394, α vs time.

Table 1 $C_{NRP_{\theta p}}$ determined experimentally for various fluid viscosities^a

Fluid description	$C_{NRP_{\theta p}}$
1,000 cSt silicone	0.054
6,700 cSt silicone	0.350
10,000 cSt silicone	0.336
32,000 cSt silicone	0.490
100,000 cSt silicone	0.676
100,000 cSt silicone (50% full)	0.781
100,000 cSt corn syrup	0.780
100,000 cSt viscoelastic	0.160

^a $p = 6000$ rpm, $\omega_1 = 500$ rpm.**Table 2** Flight test results (1978) for 155-mm liquid-filled projectiles^a

Round no.	Type of fluid	Viscosity ν , cSt	Comments
E1-9391	Corn syrup	1.92×10^5	Unstable
E1-9392	Glycerol	1.03×10^3	Stable
E1-9393	Corn syrup	1.92×10^5	Unstable
E1-9394	Corn syrup	1.92×10^5	Unstable
E1-9395	Corn syrup	2.14×10^6	Stable
E1-9396	Glycerol	6.34×10^3	Constant yaw

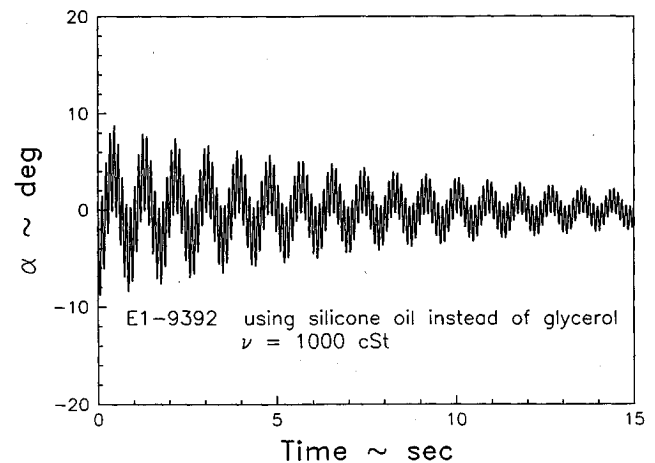
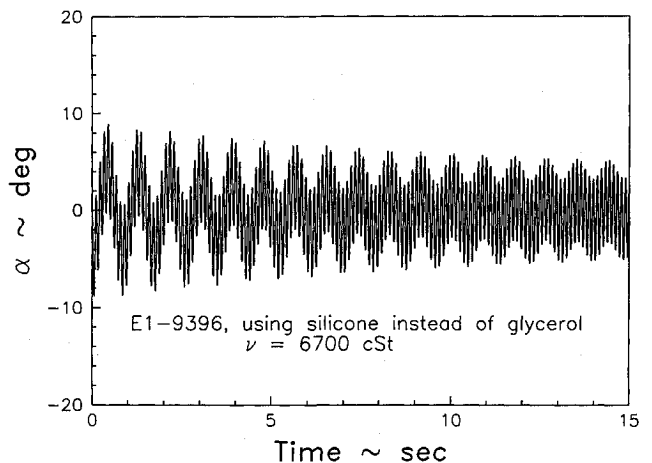
^aTransonic launch ≈ 320 m/s, initial yaw 10–12 deg; all rounds were conditioned to 22°C except for E1-9395 and E1-9396, which were conditioned to 4°C.**Table 3** Flight test results (1991) for 155-mm liquid-filled projectiles^a

Round no.	Type of fluid	Viscosity ν , cSt	Comments
1	Silicone	1.0×10^4	Unstable
2	Silicone	3.5×10^4	Unstable
3	Silicone	1.0×10^5	Unstable
4	Silicone (50% full)	1.0×10^5	Unstable
5	Viscoelastic	1.0×10^5	Stable

^aTransonic launch ≈ 320 m/s, initial yaw 10–12 deg.

Comparison of E1-9394 with the Tricyclic Theory

The yawsonde flight record from D'Amico and Miller⁹ for the unstable flight of projectile E1-9394 is shown in Fig. 3. The variable σ_N is a measure of the angular displacement with respect to the position of the sun and the velocity vector of the projectile; σ_N is analogous to the complex angle of attack used in the tricyclic theory. The associated spin rate for this round is shown in Fig. 4 as $\dot{\phi}$, which is the projectile's spin rate measured in the sun reference frame. Using test fixture results for a liquid fill of corn syrup, $C_{NRP_{\theta p}} = 0.78$ was determined. A typical simulation of a 155-mm projectile is shown in Table 4, using the flight test firing conditions and laboratory test fixture results for corn syrup. Note that the damping constants indicate that the round is stable in precession (λ_2) and unstable in nutation (λ_1). A graphical representation of these results in the angle-of-attack plane is shown in Fig. 5. By comparing Figs. 3 and 5, it can be seen that the angle-of-attack histories provide reasonable agreement up to approximately 5 s. After 5 s the two histories do not agree, but this is to be expected because of the underlying assumptions on which the tricyclic theory is based. The flight test yaw growth is much faster because of the associated rapid spin decay of the projectile (Fig. 4). As the spin rate decreases, the round becomes less stable, and thus the nutation angle increases. In the tricyclic theory, the spin rate is held constant (6000 rpm for this simulation), which provides a greater gyroscopic stability than the round actually experiences in flight. Also, after 5 s for the flight projectile, the angle of attack can no longer be considered small; thus any small angle and linear coefficient assumptions are no longer valid. However, the modified tricyclic theory does predict for these specific flight conditions that this liquid-filled projectile will experience an unstable flight. It is not intended that the modified tricyclic theory would be able to predict the actual flight motion of an unstable liquid-filled projectile. If the true flight

**Fig. 6** Tricyclic flight simulation for round E1-9392, α vs time.**Fig. 7** Tricyclic theory predictions for round E1-9396, α vs time.

motion is required, then a more sophisticated method, such as a 6-DOF simulation, would have to be employed.

Comparison of E1-9392 with the Tricyclic Theory

From the flight test results, the glycerol-filled round was stable in flight. For the tricyclic analysis, test fixture results for a 1000-cSt silicone fluid that is similar to glycerol was used to calculate $C_{NRP_{\theta p}} = 0.0535$. The tricyclic theory predicted a stable flight for round E1-9392, as shown in Fig. 6.

Comparison of E1-9396 with the Tricyclic Theory

The glycerol-filled round E1-9396 was neutrally stable throughout the flight, with a constant nutation angle. The cold conditioning of the flight projectile caused the glycerin to have the desired viscosity. It is assumed that, because of the relatively large mass of the projectile and the short time of flight, no significant changes to the temperature or viscosity of the liquid fill would occur. Test fixture data for a silicone oil with $\nu = 6700$ cSt were used in the tricyclic analysis that provided a $C_{NRP_{\theta p}} = 0.350$. The simulated α vs time plot, Fig. 7, indicates a constant nutation angle that agrees with the flight test results.

Comparison of 1991 Flight Test Results

Tricyclic simulations were performed on the projectiles listed in Table 3. For these projectiles and flight conditions, the sign and magnitude of λ_1 is a good indicator of stable or unstable flight. A large negative value of λ_1 indicates good stability, a value near 0 signifies marginal stability, and a large positive value indicates an unstable projectile. Table 5 presents λ_1 calculated from the tricy-

Table 4 Typical tricyclic simulation, initial conditions and results

Initial conditions	
$I_x = 0.176 \text{ kg-m}^2$	$\alpha_0 = 0 \text{ deg}$
$I = 1.786 \text{ kg-m}^2$	$\dot{\alpha}_0 = 0 \text{ deg/s}$
$S = 0.019 \text{ m}^2$	$\beta_0 = 0 \text{ deg}$
$d = 0.155 \text{ m}^2$	$\dot{\beta}_0 = -220 \text{ deg/s}$
$\rho = 1.055 \text{ kg/m}^3$	$V = 320 \text{ m/s}$
$C_{m\alpha} = 4.450$	$p = 6000 \text{ rpm}$
$C_{mq} = -10.00$	$\Delta t = 0.0035 \text{ s}$
$C_{n\beta p} = 0.500$	$t_{\max} = 30.00 \text{ s}$
$C_{m\delta} = 0.0$	$\delta = 0 \text{ deg}$
$C_{NRP_{\theta p}} = 0.78$	
Results	
$q = 54056. \text{ N/m}^2$	$\tau = 1.302$
$s_g = 2.44$	$K_1 = 4.618 \text{ deg}$
$\omega_1 = 523.6 \text{ rpm}$	$K_2 = 4.618 \text{ deg}$
$\omega_2 = 68.7 \text{ rpm}$	$K_3 = 0.0 \text{ deg}$
$\lambda_1 = 0.115 \text{ s}^{-1}$	$\lambda_2 = -0.109 \text{ s}^{-1}$

Table 5 Tricyclic simulation of 1991 flight test results (see Table 3)

Round no.	$C_{NRP_{\theta p}}$	λ_1	Theory ^a	Flight test ^a
1	0.336	-0.010	N	U
2	0.490	0.033	U	U
3	0.676	0.086	U	U
4	0.781	0.116	U	U
5	0.160	-0.060	S	S

^aN = neutrally stable, U = unstable, S = stable

clic theory and compares the predictions to the flight test results. The only minor discrepancy between prediction and flight test occurs for round 1 (10,000-cSt silicone fill). An unstable flight was observed during the flight test, whereas the modified tricyclic theory indicates the round should be neutrally stable. Although there is a difference between the flight test and the simulation, the prediction does correctly identify round 1 as a poor design for transonic flight because of its relatively low negative value of λ_1 . Overall, the predictions of whether a projectile would experience a stable or unstable flight were in good agreement with the flight test results for a wide range of liquid fills.

Relationship Between External and Internal Effects

The modified tricyclic theory can also be used to investigate the interrelationship between the aerodynamic characteristics and the liquid-fill effects acting on a projectile. Specifically, how do these two quantities interact to affect the stability of a projectile? From this study, an important observation was made concerning the liquid fill and the Magnus moment. For a transonic flight of a 155-mm projectile, the instability increased as the magnitude of the liquid-induced side moment increased. Instability occurred when the magnitude of the liquid-induced side moment was approximately equal to the Magnus moment. Thus, both the external and internal moments contributed equally to the stability or instability of the projectile.

Finally, it should be noted that the modified tricyclic theory is not restricted to liquid fills. Any nonrigid payload (i.e., partial solid/partial liquid, mechanical linkages, gears, etc.) can be simulated by the theory as long as a suitable value of $C_{NRP_{\theta p}}$ can be determined.

The modified tricyclic theory provides the aeroballistician and projectile designer with a useful tool to increase their understanding of the interaction between the aerodynamic and payload moments and their effect on the projectile's stability.

Conclusions

- 1) The tricyclic theory has been modified to include nonrigid payload (i.e., liquid fill) effects, which are represented by a Magnus-type side moment.
- 2) Liquid-fill effects can be determined from theory or laboratory experiments.
- 3) The modified tricyclic theory can be used to evaluate the interrelationship between the aerodynamic and liquid-fill moments to show which has the greater influence on stability.
- 4) Although the physical mechanisms producing the side moment differ between the classical Magnus and the liquid payload influences, the individual and combined effects on the projectile's dynamic stability can be quickly evaluated with this theory.
- 5) Predictions from the modified tricyclic theory show good agreement with flight test results.
- 6) The modified tricyclic theory is useful as an initial screening tool for designers of liquid-filled projectile, allowing inadequate designs to be eliminated early in the design process.

Acknowledgments

The author would like to acknowledge the following two individuals: Timothy Maust for his computer programming assistance and Miles Miller for his overall support and guidance during this study. Their help was greatly appreciated.

References

- ¹Vaughn, H. R., "A Detailed Development of the Tricyclic Theory," Sandia Lab., SC-M-67-2933, Albuquerque, NM, Feb. 1968.
- ²Miller, M. C., "Flight Instabilities of Spinning Projectiles Having Non-Rigid Payloads," *Journal of Guidance, Control, and Dynamics*, Vol. 5, No. 2, 1982, pp. 151-157.
- ³Murphy, C. H., "Angular Motion of a Spinning Projectile with a Viscous Liquid Payload," 1983, *Journal of Guidance, Control, and Dynamics*, Vol. 6, No. 4, 1983, pp. 280-286.
- ⁴Hall, P., Sedney, R., and Gerber, N., "Fluid Motion in a Spinning Coning Cylinder via Spatial Eigenfunction Expansion," U.S. Army, Ballistic Research Lab., BRL-TR-02813, Aberdeen Proving Ground, MD, Aug. 1987.
- ⁵Li, R., and Herbert, T., "Computational Study of the Flow in Spinning and Nutating Cylinders," *AIAA Journal*, Vol. 28, No. 9, 1990, pp. 1596-1604.
- ⁶Vaughn, H. R., Oberkamp, W. L., and Wolfe, W. P., "Numerical Solution for a Spinning, Nutation, Fluid-Filled Cylinder," Sandia National Lab., SAND83-1789, Albuquerque, NM, Dec. 1983.
- ⁷Rosenblat, S., Gooding, A., and Engelman, M. S., "Finite Element Calculations of Viscoelastic Fluid Flow in a Spinning and Nutating Cylinder," U.S. Army, Chemical Research, Development, and Engineering Center, CRDEC-CR-87021, Aberdeen Proving Ground, MD, Dec. 1986.
- ⁸Miller, M. C., "Laboratory Test Fixture for Non-Rigid Payloads," *Proceedings of the International Congress on Instrumentation in Aerospace Simulation Facilities-ICIASF '89*, Research Center Göttingen, Germany, Sept. 1989, pp. 350-364.
- ⁹D'Amico, W. P., and Miller, M. C., "Flight Instabilities Produced by a Rapidly Spinning, Highly Viscous Liquid," *Journal of Spacecraft and Rockets*, Vol. 16, No. 1, 1979, pp. 62-64.
- ¹⁰Miller, M. C., and Joseph, D. D., *Proceedings of the Workshop on Problems of Rotating Liquids*, U.S. Army, Chemical Research, Development, and Engineering Center, CRDEC-SP-038, Aberdeen Proving Ground, MD, July 1991, pp. 309-332.

Gerald T. Chrusciel
Associate Editor